A practical closed loop transfer function estimation method to enable better control performance

Robin De Keyser, Isabela R. Birs, Cristina I. Muresan, and Clara M. Ionescu

Abstract— **Industrial applications are often downgraded to 60% of their original performance in the first 6 months of their execution. In most processes, these are still robust to process specs and continue to be used as such. However, significant performance improvement up to 40-50% is achievable by retuning the controllers . For this, it is very relevant to have methods applicable in practice to deliver better process models to achieve better closed loop performance. In this paper, we give such a solution that is based on closed loop data, i.e. with the existing controller in operation. The measurement interval is short and the test delivers data that is highly robust to loop disturbances. The obtained process model is accurate and can be further used to design a new controller or to retune the existing one. To validate the proposed approach, two case studies are considered: a non-minimum phase integrating system and a poorly damped integrating one. The experimental results demonstrate the robustness and efficiency of this novel approach.**

I. INTRODUCTION

The Proportional-Integrative-Derivative (PID) controller [1] is still regarded as the main algorithm to control industrial processes. Although several advanced control methods have been developed, the PID is still widely used. The Model Predictive Control (MPC) approach is highly suitable to be used in industrial applications and a candidate to replace the PID since compared to the latter it can handle constraints [2]. But, much like the PID, the MPC is a model based approach. For MPC to produce excellent results, an accurate process model is required in the prediction.

The simplest and industry-friendly methods used to extract relevant process data have emerged with the popular Ziegler-Nichols methods [3]. The closed loop (CL) test implies using a P controller and driving the process to its stability limit, which could be potentially hazardous in the presence of disturbance or noise. To avoid instability, the method was replaced by the relay approach [4], with several extensions and variations developed [5], [6]. Open or close loop tests using step response data have also been proposed as alternative solutions to extract relevant process information [7], [8]. Process models were also obtained based on the impulse response [9], [10], [11]. Other alternative methods to obtain accurate or simple process models are reviewed in [12], [13] or [14]. The recurring feature of these methods is that they require a great amount of data to identify a process model, which is an important issue in industrial applications. Fast tests that require minimum production losses are preferred.

In this manuscript, a reliable and simple solution for estimating accurate higher order plus dead time (HOPDT) process models is described. A short sine signal of a chosen test frequency is applied to the process controlled by an existing known PID. The measured CL output signal is then used to estimate the impulse response of the CL system using a filtering method. Later, using discrete Fourier transform, the frequency response of the CL system is estimated in a few points around the test frequency. The corresponding process frequency response points are then computed using the known controller transfer function and further used to estimate with great accuracy a HOPDT process model. Finally, the HOPDT model is used to tune an MPC controller that replaces the existing controller and ensures better closed loop performance. To compare the results, the process frequency response is also used to tune PID controllers. The experimental results obtained for two very different processes show that the proposed methodology leads to accurate process models that can be used successfully to tune MPC/PID controllers. Compared to existing modeling techniques, the method proposed in this paper is short, accurate and suitable for both open and closed loop tests. Compared to other test signals commonly used in system identification, such as chirp, multi-sine or the pseudo-random binary sequences, the proposed method uses a sine signal, which is much easier to design for users in industry who are not experts in signal processing techniques. The choice of the sine signal is optimal since it ensures that the frequency response is accurately estimated even in the presence of noise and disturbances.

The manuscript is organized in 5 parts. Section II details the closed loop method to determine the HOPDT model. Section III demonstrates the robustness of the approach. Section IV presents two case studies and the experimental validation of the proposed methodology. The conclusions are included in the last section.

This work was supported by a grant of the Romanian Ministry of Research, Innovation and Digitization, PNRR-III-C9-2022 – I8, grant number 760068/23.05.2023 and project number PN-IV-P2-2.1-TE-2023-0831, within PNCDI IV. This work was funded in part by the European Research Council (ERC) Consolidator Grant AMICAS, grant agreement No. 101043225, 2022-2027. Funded by the European Union. Views and opinions expressed are however those of the author(s) only and do not necessarily reflect those of the Euro- pean Union or the European Research Council Executive Agency. Neither the European Union nor the granting authority can be held responsible for them.

Robin De Keyser, Isabela R. Birs and Clara M. Ionescu are with the Department of Electromechanical, Systems and Metal Engineering Flanders Make EEDT Core lab, Ghent University, Tech Lane Science Park 125 and 131, 9052, Gent, Belgium Robain.DeKeyser@ugent.be, ClaraMihaela.Ionescu@ugent.be

Cristina I. Muresan and Isabela R. Birs are with the Department of Automation Technical University of Cluj Napoca, Memorandumului nr 28, 400114 Cluj-Napoca, Romania Cristina.Muresan@aut.utcluj.ro, Isabela.Birs@aut.utcluj.ro

II. Design Methodology

The following assumptions hold:

1) The transfer function $P(s)$ of the process is unknown.
2) A test frequency $\bar{\omega}$ is selected. The process critical frequency is a good choice; this can be easily detected with a relay test. Detailed information regarding the relay test can be found in [4].
3) A controller is used to stabilize the process and its transfer function $C(s)$ is fully known.
4) The settling time (ST) is known or has been estimated experimentally.

First, two signals are defined as the impulse response (IR)-explorer and the IR-extractor, with an example given in Fig. 1. The IR-explorer is a signal $u(t)$ that contains 4 sections, indicated by the red arrows in the upper plot of Fig. 1. These 4 sections can be repeated if needed.

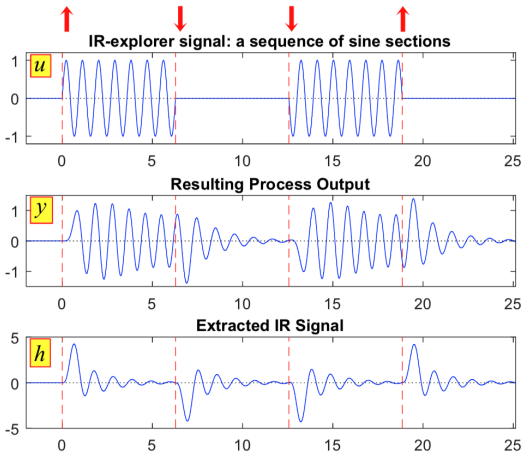

Fig. 1. The IR-explorer, resulting output $y(t)$ and IR-extractor signals. Red arrows indicate the 4 sections of the the test signal

The IR-explorer signal $u(t)$ is obtained as a sum of 4 sine signals with the same frequency $\bar{\omega}$. The first and the fourth sine signals are positive ones, while the second and third signals are negative sines. The direction of the red arrows in the upper plot of Fig. 1 suggests the sign of the sine signals. Each sine signal is delayed by approximately ST seconds compared to the previous one, such that an integer number of sinusoidal periods is obtained in each section. Then, summing up all 4 sine signals leads to the final IR-explorer signal $u(t)$ as indicated in the upper plot of Fig. 1.

As it will be further shown, each of these sine signals produces either a positive or negative impulse response. Delaying the sine signals by more than ST can be possible, but it will not produce any more data regarding the process as the IR coefficients will decay to zero afterwards. The resulting IR signals are indicated in Fig. 1 lower plot. For accurate estimations of the IR signal, these 4 signals are averaged. In case of noisy signals, a repetition of the 4 sections in the signal $u(t)$ will reduce the signal to noise ratio and will provide for a better IR signal estimation.

Once the signal $u(t)$ has been properly designed and applied to the input of the process, the output is measured and further used to estimate the process IR. The estimation is based on a simple and efficient method indicated in Fig. 2. Assume here that the Laplace transform of the test signal $u(t)$ is denoted as $F(s)$, since $U(s) = F(s)\Delta(s)$, where $\Delta(s) = 1$, since $\delta(t)$ is the Dirac impulse. The test signal $u(t)$ is applied to the input of the closed loop system, denoted as $T(s)$ and thus $Y(s) = T(s)U(s)$, according to the upper block diagram in Fig. 2. Then, swapping the $T(s)$ and $F(s)$ blocks leads to the lower diagram in Fig. 2. This time, the Dirac impulse is applied (theoretically) to the input of $T(s)$ resulting in the real IR, denoted as $h(t)$. This is further fed to the filter $F(s)$ and this results in the output $y(t)$ of the closed loop system (similarly to the upper block diagram). The simplicity of the methodology resides from here: further filtering of the output $y(t)$ with the filter $\frac{1}{F(s)}$ leads to an estimation of the IR of the closed loop system, denoted as $\hat{h}(t)$. As indicated in Fig. 1, for each section of the input $u(t)$ an estimation of IR is obtained. The final process IR is obtained by averaging over all IR estimations.

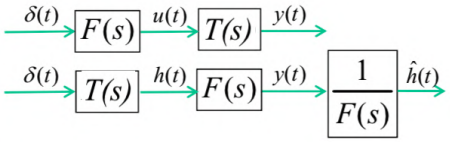

Fig. 2. Block diagram to obtain the process impulse response

Remark 1: In practice, $u(t)$ is applied to the input of the closed loop system. The output $y(t)$ is measured and then used to estimate the IR $\hat{h}(t)$ using the inverse of the filter $F(s)$. In noisy free situations, $h(t) = \hat{h}(t)$.

Remark 2: The amplitude of the signal $u(t)$ should be chosen such that the output of the closed loop system avoids saturation or reaching safety limits.

The next step consists in calculating the frequency response of the closed loop system, $T(j\omega)$, in a few points around the test frequency (e.g. $\omega_i = 0.80\bar{\omega}, 0.85\bar{\omega}, ..., \bar{\omega}, ..., 1.15\bar{\omega}, 1.20\bar{\omega}$). This is done using the DFT:

$$T(j\omega) = \int_0^\infty h(t)e^{-j\omega t}dt \tag{1}$$

$$T_i = T(j\omega_i) \cong T_s \sum_{k=0}^{N_s-1} h_k e^{-j\Omega_i k} \tag{2}$$

where N_s is the number of measured samples and T_s is the sampling period with $t = kT_s$, $h_k = h(kT_s)$ and $\Omega_i = \omega_i T_s$ is the constant discrete frequency.

For each frequency ω_i, the frequency response point C_i of the controller can be easily computed since the controller transfer function is completely known (Assumption 3 above). The process $P_i = P(j\omega_i)$ frequency response points can be determined based on:

$$P_i = P(j\omega_i) = \frac{T(j\omega_i)}{C(j\omega_i)(1-T(j\omega_i))} \tag{3}$$

The complex numbers P_i are further used to estimate a HOPDT transfer function, denoted as $M(s)$:

$$M(s) = \frac{b_{N_b}s^{N_b} + ... + b_1 s + b_0}{a_{N_a}s^{N_a} + ... + a_1 s + 1} e^{-\tau s} \tag{4}$$

where b_0 is the static gain and assumed to be fully known, τ is the time delay, N_a and N_b are the number of poles and zeros, with $N_a > N_b$. To estimate the HOPDT parameters in (4) the standard Non Linear Least Squares (NLLS) algorithm is used and defined as:

$$\{\tau^*, \theta^*\} = arg\min_{\tau,\theta} V(\tau, \theta) \tag{5}$$

where $\theta = [a_1 a_2 ... a_{N_a} | b_1 b_2 ... b_{N_b}]$, with the cost function $V(\tau, \theta)$ to be minimized given as:

$$V(\tau, \theta) = \sum_i |P(j\omega_i) - M(j\omega_i)|^2 \tag{6}$$

The NLLS algorithm is implemented using the Matlab function *lsqnonlin*. The method is repeated for several (reasonable) values of the orders (N_a, N_b), each of them leading to an optimal cost $V^*(N_a, N_b)$; the final order selection for the HOPDT model is then based on the comparison of these V^* values. To solve the LS problem, the number of points P_i should be larger than $\frac{N_a+N_b}{2}$. Practice shows that convergence is fast and choosing much more points than necessary is of no real benefit. The method has been further described and tested on many simulated examples in [15].

III. A Robust Choice Of The Filter $F(s)$

In what follows, we show that the filter $F(s)$ used to estimate the process IR can be chosen in a robust way to ensure accurate estimation of the frequency response points T_i. Assume that noise and disturbances affect the output $y(t)$. These are considered hereafter as stochastic disturbances $d(t)$ modeled as colored noise with zero mean value. The output is then:

$$Y(s) = T(s)U(s) + D(s) \tag{7}$$

with $D(s)$ defined as the Laplace transform of the disturbance $d(t)$.

The estimated IR $\bar{H}(s)$ of the process is then computed, according to Fig. 2:

$$\bar{H}(s) = \frac{1}{F(s)}Y(s) = \frac{1}{F(s)}[D(s) + T(s)U(s)] \tag{8}$$

which leads to

$$\bar{H}(s) = \frac{1}{F(s)}D(s) + \frac{1}{F(s)}T(s)F(s)\Delta(s) = \frac{1}{F(s)}D(s) + H(s) \tag{9}$$

According to (9), the accuracy of the estimation is affected by the disturbance. However, an adequate choice for the filter $F(s)$ can limit the effect of the disturbance around $\bar{\omega}$. As it has been shown in Section II, the filter $F(s)$ is in fact the Laplace transform of the input $u(t)$. Since $u(t)$ is a sine signal of the test frequency $\bar{\omega}$, then:

$$F(s) = \frac{\bar{\omega}}{s^2 + \bar{\omega}^2} \tag{10}$$

The inverse of $F(s)$ is then given as:

$$F^{-1}(s) = \frac{s^2 + \bar{\omega}^2}{\bar{\omega}} \tag{11}$$

with the magnitude computed at the test frequency $\bar{\omega}$:

$$|F^{-1}(j\bar{\omega})| = \frac{-\bar{\omega}^2 + \bar{\omega}^2}{\bar{\omega}} = 0 \tag{12}$$

which clearly shows that this choice for the filter $F(s)$ effectively limits the disturbances around the test frequency $\bar{\omega}$. Thus, the filter is robust and ensures accurate estimation of the IR at the test frequency $\bar{\omega}$.

For comparison, if a step signal is used instead for $u(t)$, the filter would be given by:

$$F(s) = \frac{1}{s} \tag{13}$$

with the inverse defined as $\frac{1}{F(s)} = s$ and the corresponding magnitude at the test frequency $|F^{-1}(j\bar{\omega})| = \bar{\omega}$. In this case, the disturbance is not eliminated.

Remark: The sinusoidal test signal $u(t)$ is used to produce accurate estimations at the test frequency and close to it, in a total of 9 frequency points $0.8\bar{\omega} \leq \omega_i \leq 1.2\bar{\omega}$. Fig. 3 shows the magnitude plots of the two inverse filters previously discussed. It is obvious from here, that good estimations can be obtained around the frequency of interest using the sine test signal, compared to the step test signal.

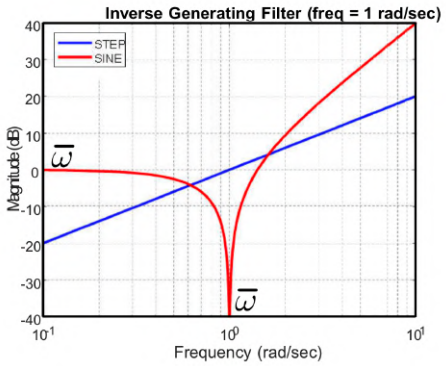

Fig. 3. Magnitude plot of $F^{-1}(j\omega)$ corresponding to step and sine signals

IV. Experimental Results

Two different types of processes are considered. The first one consists in the Quanser 2-tank system, a non-minimum phase integrating process. The second one is a high order poorly damped integrating mass-spring-damper system. In both cases, a P controller is first used to stabilize the process. Then, a test signal $u(t)$ is applied as the stepoint to closed loop system to estimate a few process frequency response

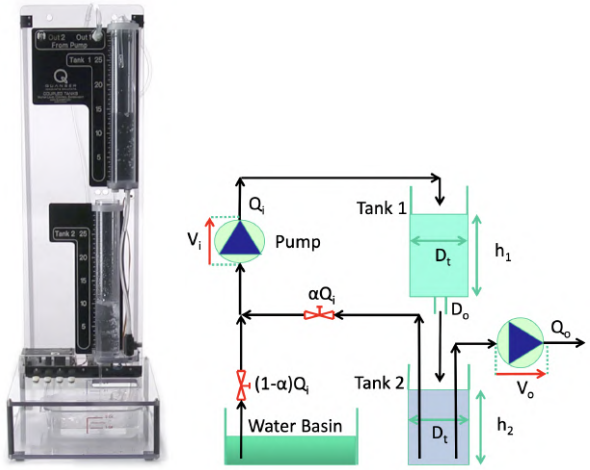

Fig. 4. a) left - The Quanser two-tank coupled system used as a case study b) right - The schematic diagram of the Quanser two-tank coupled system

points according to the proposed methodology from Section II.

A. Case study: coupled two-tank system

The process considered in this first case study is the coupled-tank system built by Quanser and given in Fig. 4 a), with the schematic diagram in Fig.4 b). The input signal is the pump flow $u(t) = V_i(t)$, while the output $y(t) = h_2(t))$ is considered to be the water level in Tank 2, at the bottom. A second pump is used to extract water from Tank 2. The resulting water flow is considered as an output disturbance $d(t) = V_o(t)$. Theoretical insight regarding the governing equations that link the input flow to the level in Tank 2 suggests that this process is non-minimum phase and integrating [16]. In order to apply the methodology described in Section II, the process is stabilized using a P controller with the proportional gain $k_p = 0.2$. The test frequency is chosen as $\bar{\omega} = 0.042$ rad/s (the process critical frequency i.e. $\angle P(j\bar{\omega}) = -180^o$).

Next, the input signal $u(t)$ is constructed using the approach in Section II and applied as the setpoint of the closed loop system. The process is affected by disturbances and noise. Two test sequences are used to reduce the signal-to-noise-ratio and allow for a better estimation of the IR. The applied input sequence $u(t)$ is given in Fig. 5, upper plot.

The measured output of the closed loop system is given in Fig. 5 middle plot. The filter $F(s)$ is constructed as:

$$F(s) = \frac{0.042}{s^2 + 0.042^2} \tag{14}$$

and its inverse is used to produce the estimated (extracted) IR response given in Fig. 5 lower plot. The real unit IR of the closed loop system is also given in this plot for comparative purposes and has been obtained using a theoretical model of the two-tank system [16]. The extracted IR is then used to compute the frequency response points of T_i using (2), which in turn are employed in the estimation of the process frequency response points P_i based on (3), where $C(j\omega_i) =$

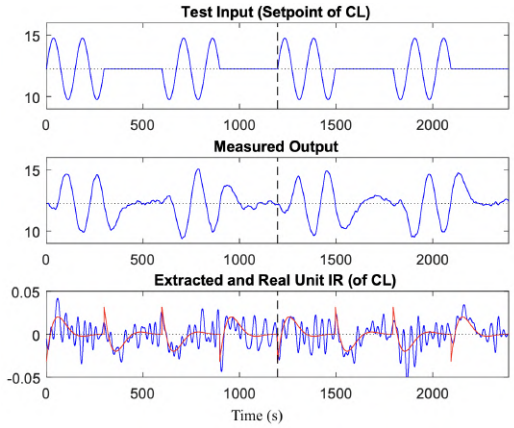

Fig. 5. The test sequence, measured output, real (red line) and estimated (blue line) IR for the two-tank system

0.2. The result of the NLLS algorithm leads to the following process transfer function:

$$P(s) = \frac{-0.164s + 0.00461}{s(s + 0.0678)} e^{-s} \tag{15}$$

Fig. 6 shows the Nyquist plots of the estimated HOPDT model in (15) and the theoretical model of the two-tank system. The frequency response points are also included. The comparative results show that the methodology has produced an accurate estimation of the process frequency response points and process model.

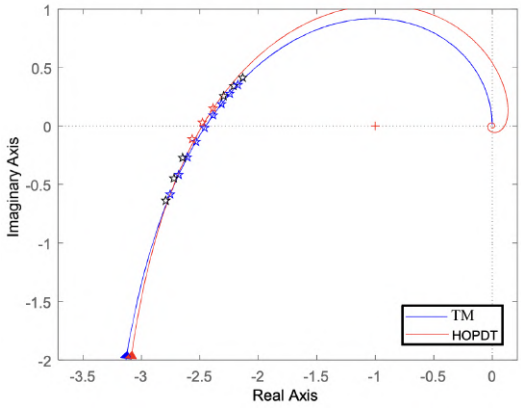

Fig. 6. The Nyquist plots and 9 frequency response points for the theoretical model (TM) and the estimated model (HOPDT) using the proposed methodology for the two-tank system

A MPC controller is now designed to control the level in Tank 2. The estimated mathematical model in (15) is used as the prediction model in the Extended Prediction Self Adaptive Control (EPSAC) approach [17]. For comparison purposes, an autotuning method is used to tune a PID controller with proportional gain $k_p = 0.22$, integral and derivative time constants $T_i = 122$ and $T_d = 16$ [16]. The closed loop results with the EPSAC controller and the PID are given in Fig. 7, for both reference tracking and disturbance rejection. The results show that the MPC

manages to achieve better closed loop performance with no overshoot and a faster settling time. The drawback is that it requires a good prediction model that should be easily obtained to be worthwhile. Using the proposed methodology in Section II, obtaining such a model is not an issue.

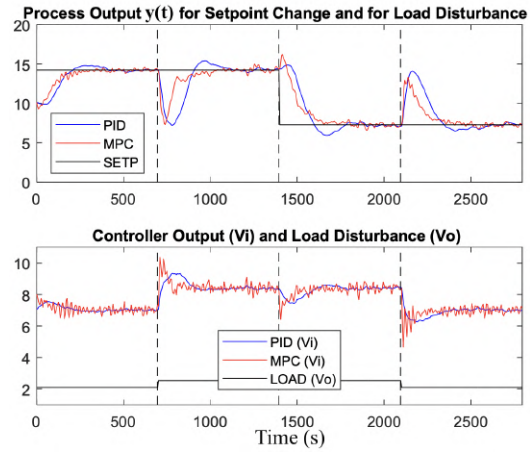

Fig. 7. Comparative closed loop results using the MPC vs the PID for the two-tank system

B. Case study: the mass-spring-damper system

The second case study considered in this paper is the mass-spring-damper (MSD) pilot plant given in fig. 8. It has one input, the voltage to the motor u(t) and two outputs, the positions of the two masses (M1 and M2) measured by the encoders. The driving force executed by the motor is the actuator and it is proportional to the input voltage u(t). It is directly acting on M1. If we are interested to control the position of M1, actuator and sensor are thus both on the same mass; this is called collocated control. If we are interested to control the position of M2, actuator and sensor are on different masses; this is called non-collocated control. Non-collocated control is much more difficult than collocated control. In the current example the focus is on the control of M2, thus non-collocated control. The position of mass M2 is denoted as $y(t)$. The 1st and the 3rd springs have been disconnected, which turns this setup into an integrating system.

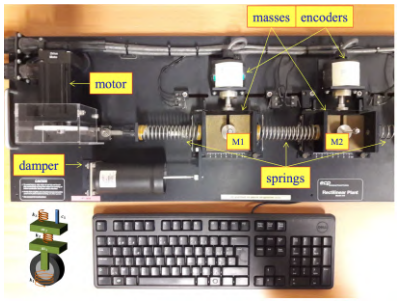

Fig. 8. The MSD used in the second case study

In order to apply the methodology described in Section II, the process is first stabilized using a simple proportional controller with $k_p = 0.1$. The test frequency is selected to be $\bar{\omega} = 9$ rad/s. Stochastic disturbances affect the system. To improve the signal-to-noise-ratio, two test sequences have been applied at the input of the closed loop system. The test signal $u(t)$ is given in Fig. 9, upper plot. The measured output $y(t)$ of the CL system is given in the same figure, middle plot. The real IR of the closed loop system is displayed in the lower plot and has been obtained using a theoretical model of the MSD system. To produce the extracted (estimated) IR, the inverse of the filter in (16) is used:

$$F(s) = \frac{9}{s^2 + 9^2} \tag{16}$$

Notice in this case that the real and estimated IR are quite similar.

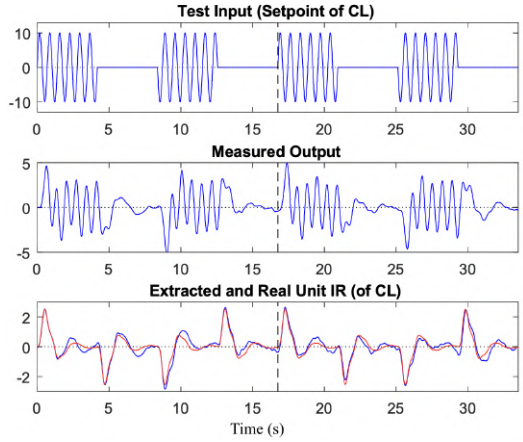

Fig. 9. The test sequence, measured output, real (red line) and estimated (blue line) IR for the MSD system

The extracted IR is then used to estimate 9 frequency response points of T_i using (2), which in turn are utilized to compute the process frequency response points P_i based on (3), where $C(j\omega_i) = 0.1$. The result of the NLLS algorithm leads to the following process transfer function:

$$P(s) = \frac{10087}{s(s+2.61)(s^2+2.53s+125)} e^{-0.08s} \tag{17}$$

Fig. 10 shows the Nyquist plots of the estimated HOPDT model in (17) and the theoretical model of the MSD. The 9 frequency response points are also included. The comparative results show that the methodology has produced accurate estimations of the frequency response points and consequently of the process model.

The MPC is now designed to control the position $y(t)$. The estimated mathematical model in (17) is used as the prediction model. The EPSAC approach is used here, as well [17]. For comparison purposes, a PID controller is also designed using the FRtool [18], with the parameters: $k_p = 0.09$, $T_i = 2.2$ and $T_d = 0.18$. The closed loop results with the EPSAC controller and the PID are given in Fig. 11. The results show that the MPC manages to achieve better closed loop performance with less output oscillations and a faster settling time. The drawback is that it requires a

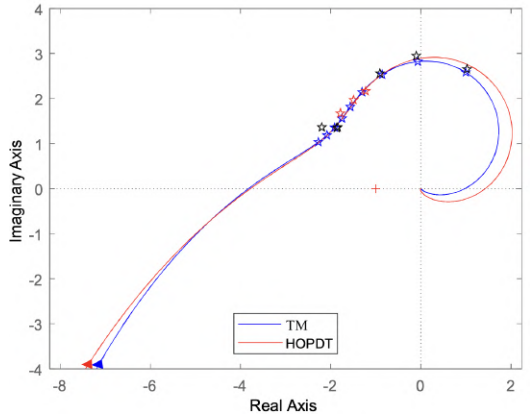

Fig. 10. The Nyquist plots and 9 frequency response points for the theoretical model (TM) and the estimated model (HOPDT) using the proposed methodology for the MSD system

good prediction model that should be easily obtained to be worthwhile. Using the proposed methodology in Section II, obtaining such a model is not an issue.

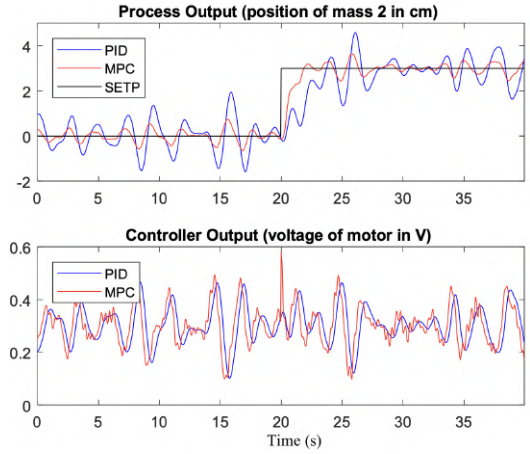

Fig. 11. Comparative closed loop results using the MPC vs the PID for the MSD system

V. CONCLUSIONS

Process models are usually difficult to obtain and time consuming, although they endorse optimally tuned controllers. Industry is primarily interested in shortcuts to obtain accurate process models in a fast and inexpensive manner.

In this paper, relevant process information was obtained using a closed loop test, with an existing controller in operation. The only requirement is that the currently operating controller transfer function is completely known – but this is usually the case as this is designed/tuned by the process operator. In this context, limited changes to industrial loops are required to obtain the process data, which is a major advantage of the proposed novel approach. Additionally, the test is short and minimally invasive and does not require shutting down the plant.

The proposed short sine test estimates first the IR of the closed loop system and its frequency response at a few frequencies close to the test frequency. Using the known controller transfer function, the process frequency response in these points can be estimated and later used to determine accurately a HOPDT model. The method is robust to disturbances, and the HOPDT model has great accuracy. MPC has the potential to replace the PID in industrial applications, but accurate models are needed in the prediction step. In this paper, the use of MPC is enhanced by obtaining accurate HOPDT prediction models in a fast and reliable way. As such, the proposed methodology aids to a wider acceptance of the MPC as a control solution in industrial applications.

REFERENCES

[1] K. Åström and T. Hägglund, "Revisiting the ziegler–nichols step response method for pid control," *Journal of Process Control*, vol. 14, no. 6, pp. 635–650, 2004.

[2] A. Aboelhassan, M. Abdelgeliel, E. E. Zakzouk, and M. Galea, "Design and implementation of model predictive control based pid controller for industrial applications," *Energies*, vol. 13, no. 24, id 6594, 2020.

[3] J. G. Ziegler and N. B. Nichols, "Optimum Settings for Automatic Controllers," *Transactions of the ASME*, vol. 64, pp. 759–76, 1942.

[4] K. Åström and T. Hägglund, "Automatic tuning of simple regulators with specifications on phase and amplitude margins," *Automatica*, vol. 20, no. 5, pp. 645–651, 1984.

[5] C. A. Monje, B. M. Vinagre, V. Feliu, and Y. Chen, "Tuning and auto-tuning of fractional order controllers for industry applications," *Control Engineering Practice*, vol. 16, no. 7, pp. 798–812, 2008.

[6] K. Tan, T. Lee, and Q. Wang, "Enhanced automatic tuning procedure for process control of pi/pid controllers," *AlChE Journal*, vol. 42, no. 9, pp. 2555–2562, 1996.

[7] R. De Keyser and C. I. Muresan, "Robust estimation of a sopdt model from highly corrupted step response data," *2019 18th European Control Conference*, pp. 818–823, 25-28 June 2019, Naples, Italy.

[8] W. Jianhong and R. A. Ramirez-Mendoza, "The practical analysis for closed-loop system identification," *Cogent Engineering*, vol. 7, no. 1, p. 1796895, 2020.

[9] D.-F. Xu, L. and E. Yang, "Separable recursive gradient algorithm for dynamical systems based on the impulse response signals," *Int. J. Control Autom. Syst.*, vol. 18, p. 3167–3177, 2020.

[10] L. Xu and F. Ding, "Parameter estimation for control systems based on impulse responses," *Int. J. Control Autom. Syst.*, vol. 15, pp. 2451–2479, 2017.

[11] L. Xu, F. Ding, and Q. Zhu, "Decomposition strategy-based hierarchical least mean square algorithm for control systems from the impulse responses," *International Journal of Systems Science*, vol. 52, no. 9, pp. 1806–1821, 2021.

[12] L. Ljung, T. Chen, and B. Mu, "A shift in paradigm for system identification," *International Journal of Control*, vol. 93, pp. 173–180, 2020.

[13] P. Albertos, "Industrial process identification and control design: step-test and relay-experiment-based methods [book review]," *IEEE Control Systems Magazine*, vol. 34, no. 2, pp. 78–80, 2014.

[14] T. Liu, Q.-G. Wang, and H.-P. Huang, "A tutorial review on process identification from step or relay feedback test," *Journal of Process Control*, vol. 23, no. 10, pp. 1597–1623, 2013.

[15] R. De Keyser, I. R. Birs, C. I. Muresan, and C. M. Ionescu, "A practical approach for transfer function estimation using short, transient process data," *IFAC-PapersOnLine*, vol. 58, no. 15, pp. 426–431, 2024, 20th IFAC Symposium on System Identification SYSID 2024.

[16] R. De Keyser and C. I. Muresan, "Validation of the kc autotuning principle on a multi-tank pilot process," *IFAC-PapersOnLine*, vol. 52, no. 1, pp. 178–183, 2019.

[17] R. De Keyser, "Model based predictive control for linear systems," *UNESCO Encyclopaedia of Life Support Systems Robotics and Automation*, vol. XI, p. Contribution 6.43.16.1, 2003, Eolss Publishers Co Ltd.: Oxford, UK.

[18] C. M. Ionescu and R. De Keyser, "The next generation of relay-based pid autotuners (part 1): Some insights on the performance of simple relay-based pid autotuners," *IFAC Proceedings Volumes*, vol. 45, no. 3, pp. 122–127, 2012.